Loss and Permeability Dependence on Temperature in Soft Ferrites

Fausto Fiorillo[1], Cinzia Beatrice[1], Marco Coïsson[1], and Ljubov Zhemchuzhna[2]

[1]Istituto Nazionale di Ricerca Metrologica (INRIM), 10135 Torino, Italy
[2]Dipartimento di Ingegneria Elettrica, Politecnico di Torino, 10129 Torino, Italy

Wideband energy loss and permeability behavior of Mn–Zn and Ni–Zn ferrite ring cores has been investigated between 2 and 50 mT up to 140 °C. The measurements have been performed by a fluxmetric method from direct current (dc) to 10 MHz and by a transmission line method from a few 10^5 Hz to 1 GHz. While magnetic softening upon heating from room temperature always occurs at low frequencies, mixed behavior is observed, depending on the polarization value, on approaching the megahertz range. The loss versus frequency curves at different temperatures tend to coalesce towards the microwave regime. The overall loss and permeability properties are interpreted recognizing the separate roles of domain wall (DW) and rotational processes and their frequency dependence. Weakening of the magnetocrystalline anisotropy with temperature leads to reduced DW dissipation, while affecting the spectral distribution of the damped spin precessional frequencies. Eddy current mechanisms are not involved in such phenomena. Dissipation effects by DWs and rotations are prevalent in the lower and upper range of frequencies, respectively. This feature is quantitatively interpreted generalizing concepts and methods of the statistical theory of losses.

Index Terms—**Initial permeability, magnetic losses, soft ferrites, spin damping.**

I. Introduction

THE magnetic properties of soft ferrites are tailored to good extent by finely acting on their composition, so that anisotropy compensation may lead to the softest behavior upon the temperature range useful for specific applications [1], [2]. Since optimization is pursued in as wide a frequency band as possible, a compromise between the conflicting requirements of high permeability and high cutoff frequency (Snoek's rule) must be reached, under the additional correlated constraint of loss minimization. This calls for an investigation of the domain wall (DW) processes and the rotations, discriminating between their separate contributions to loss and permeability as a function of frequency. On changing the temperature, such contributions will expectedly follow different routes. Literature results show that the power losses, measured as a function of temperature, pass through a minimum value, whose depth and position depends on the magnetizing frequency in a somewhat unexplained fashion [3]–[5]. Lack of interpretation appears to derive to some extent from certain measuring limitations, like a restricted experimental frequency band, hindering meaningful analysis [3], [6], [7]. Theoretical deficit may lead to crude loss decomposition procedures, where hardly justified anomaly factors are invoked to reconcile predictions and experiments [3], [8].

In this paper, we present significant results on the wideband permeability and energy loss dependence on temperature (23 °C–140 °C) in sintered Mn–Zn and Ni–Zn ferrite ring samples. It is shown that, following the evolution of the anisotropy energy, the loss decreases and the permeability increases with temperature in both materials in the lower range of frequencies (up to some 10^5–10^6 Hz, depending on the value of the peak polarization J_p). In the upper frequency range, up to 1 GHz, minor variations of the loss figure are found. We show that combined analysis of loss and permeability can be performed applying the concept of loss separation under very general terms, independent of the specific dissipation mechanism. In this way, one is able to discriminate between DW and rotational contributions to the energy losses [9], [10]. The DW processes, in particular, appear to exhibit pure relaxation behavior, while rotations find distributed resonating conditions, all influenced by the temperature induced change of the anisotropy energy. In the following, we will concentrate on results obtained up to $J_p = 50$ mT, where we fall into the Rayleigh range and we can provide meaning to a direct relationship between energy loss and complex permeability.

II. Experimental Method and Results

Commercial ring samples of Mn–Zn (N87) and Ni–Zn (4A11) sintered ferrites were characterized between direct current (dc) and 10 MHz using a calibrated hysteresisgraph wattmeter and from 100 kHz to 1 GHz by means of a coaxial line method. The samples had outside diameter and thickness in the ranges 15–10 mm and 5.3–4.04 mm, respectively. Additional measurements were performed on samples progressively thinned down to 1.2 mm. The hysteresisgraph setup was built, according to conventional schemes [11], around an Agilent 33220A function generator, an NF-HSA4101 power amplifier (DC-10 MHz, 50 VA), a four-channel variable resolution (14–8 b) 500 Msample/s TDS 714L oscilloscope, and, at the lowest frequencies, a couple of SR560 low-noise signal amplifiers. The dc characterization included the initial magnetization curve, with the associated determination of the Rayleigh parameters a and b. Knowledge of these parameters permits us, in the investigated induction range, to separate the reversible and irreversible contributions to J_p, the latter being exclusively due to the DW processes. The ring sample, endowed with bifilar windings having number of turns, wire diameter, and length of the connecting leads appropriate to the specific test frequency, is placed into a nylon cylindrical holder, fastened to a heating resistor. The measuring temperature is obtained by a copper-constant microjunction stuck onto the sample surface.

Manuscript received March 07, 2009. Current version published September 18, 2009. Corresponding author: F. Fiorillo (e-mail: f.fiorillo@inrim.it).

Color versions of one or more of the figures in this paper are available online at http://ieeexplore.ieee.org.

Digital Object Identifier 10.1109/TMAG.2009.2025049

The complex permeability was determined up to 1 GHz by placing the ring sample under test against the short-circuited bottom of a 50 Ω coaxial line energized by an Agilent 8753A network analyzer. The measurement directly provides the complex scattering parameter $S_{11} = S'_{11} + jS''_{11}$ at the sample plane. This is related by standard formulas to the real and imaginary parts of the line impedance $Z_{\rm in}$ at the same plane. By repeating the measurement with and without the sample and taking the difference $\Delta Z_{\rm in}$, the real μ' and imaginary μ'' permeability components of the ferrite sample versus frequency are obtained [12]. The need for consistent wideband measurements is in this way satisfied, because the results of the two measuring methods can be compared upon an overlapping intermediate frequency interval. A limit is, however, apparent, because the fluxmetric and coaxial line measurements are performed at given J_p and constant irradiated power, respectively. Coaxial line experiments made at different defined J_p values upon partially overlapping frequency intervals show, however, that μ' and μ'' become to a very good extent independent of J_p beyond a sufficiently high frequency f_o. The physical reason for this behavior is found in the largely predominant role played by the rotations at frequencies higher than f_o. By combination of the two measuring methods, we thus attain the complete energy loss versus frequency behavior at given J_p value in the considered 2–50-mT interval. The loss figure directly measured in the lower frequency range with the fluxmetric method will in fact be combined with the one calculated in the upper frequency range from the measured permeability

$$W(f) = \pi J_{\rm p}^2 \mu''/(\mu'^2 + \mu''^2). \tag{1}$$

An example of wideband permeability behavior measured in a Mn–Zn ring sample at 23 °C and 100 °C is offered in Fig. 1. It shows a strong increase of permeability with temperature in the lower range of frequencies and a corresponding leftward shift of the resonance peak. The low-frequency softening is the obvious result of decreased anisotropy energy, making rotations and DW displacements easier and leading to the loss results shown in Fig. 2. It is noticed how the remarkable drop of the loss figure following an increase of temperature tends to vanish at high frequencies, in association with the disappearance of the DW processes. Such a transition is apparent in the behavior of the energy loss versus frequency $W(f)$ curves presented in Figs. 3 and 4. Similar response is observed in the Ni–Zn samples, as illustrated in Figs. 5 and 6. It is stressed, however, that certain types of Ni–Zn ferrites (not shown here) are affected by relevant magnetic viscosity phenomena, which, being thermally activated, may engender a somewhat anomalous dependence of loss and permeability on temperature. It thus appears that the often remarked steep increase of the loss displayed by ferrites on approaching the megahertz range, generally lumped in the literature into a residual loss term, marks the transition to the regime where the permeability becomes fully rotational [8].

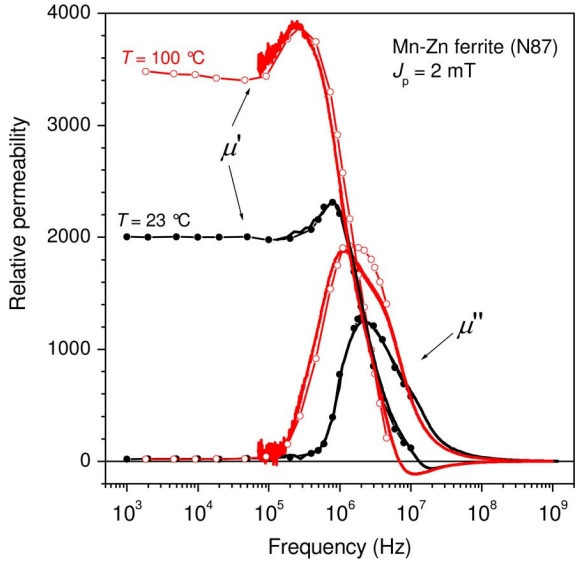

Fig. 1. Wideband real and imaginary permeability dependence on frequency in a Mn–Zn ferrite ring sample at $J_p = 2$ mT and two temperatures. Symbols: fluxmetric method (up to 10 MHz). Solid lines: coaxial line method.

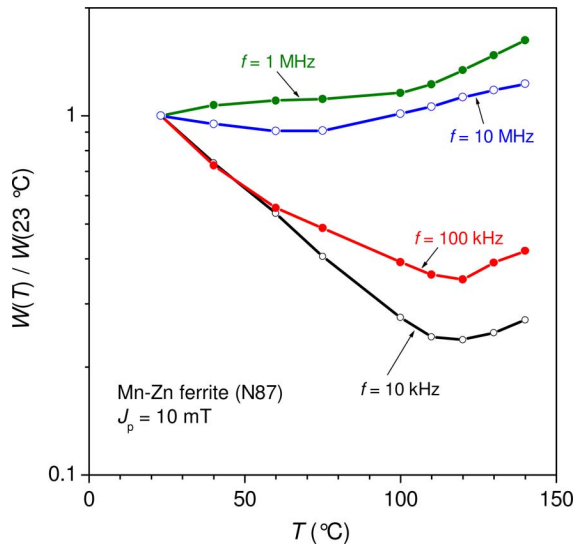

Fig. 2. Reduced energy loss $W(T)/W$ (23 °C) versus temperature T in a Mn–Zn ferrite ring sample for given peak polarization value $J_p = 10$ mT and four different magnetizing frequencies.

III. Discussion

In order to provide a quantitative interpretation of the loss and permeability results, we find a way to distinguish between the two base magnetization processes, DW displacements and rotations, and the related dissipation mechanisms. Remarkably, we can state that eddy-current phenomena can be safely disregarded in the present samples in all the investigated frequency range. This is the conclusion of a numerical approach to the eddy current losses in these heterogeneous materials, which exploits the measured dependence of the material resistivity on frequency [13]. It is a result proved by the fact that no variation of the loss figure can be found, within the experimental uncertainty, upon progressive sample thinning. Therefore, we consider the alternative dissipation mechanism by spin damping, as lumped into the Landau–Lifshitz constant $\alpha_{\rm LL}$. The frictional effects on the DW displacements are responsible for the hysteresis loss component W_h, which is experimentally extracted from the $W(f)$

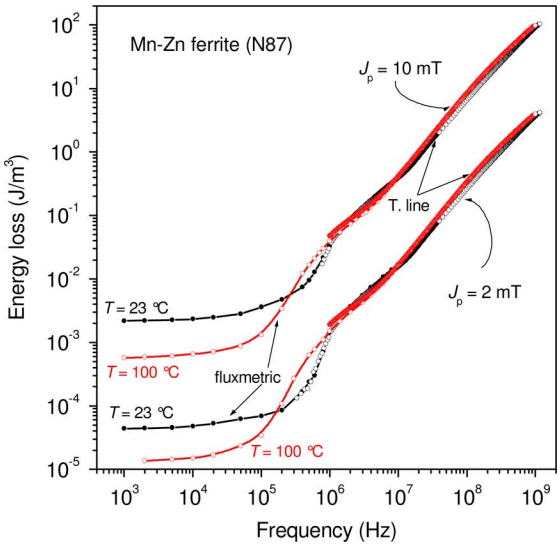

Fig. 3. Specific energy loss $W(f)$ versus frequency in the Mn–Zn ferrite, as obtained with the fluxmetric and transmission line methods at two temperatures and two J_p values. The region between 1 and 10 MHz is here covered with both methods.

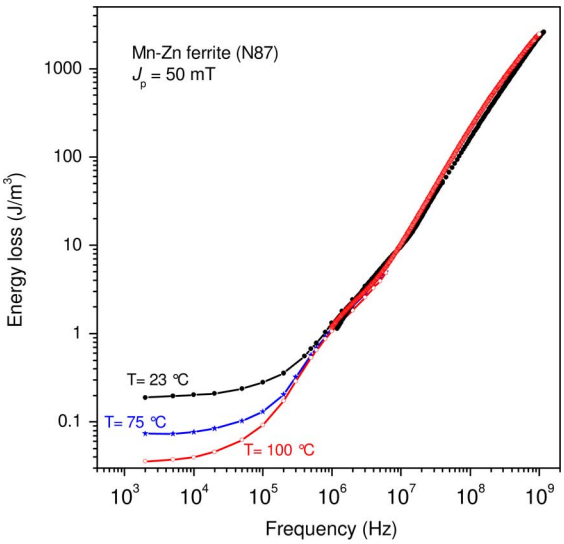

Fig. 4. Specific energy loss in the same sample of Fig. 3 for $J_p = 50$ mT.

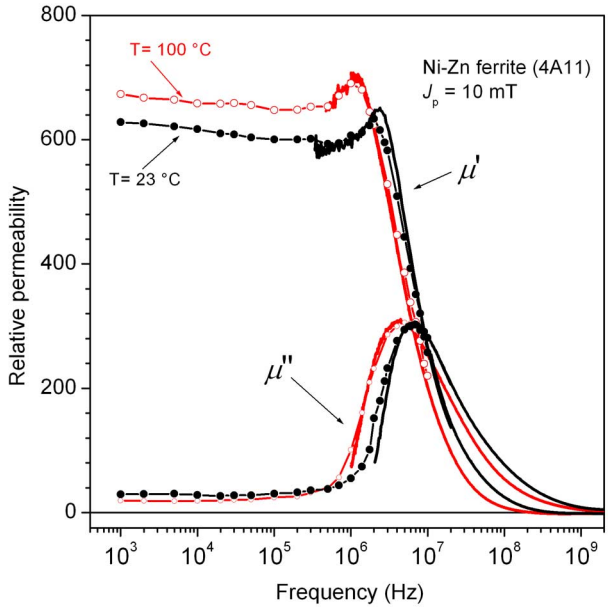

Fig. 5. Real and imaginary permeability at $T = 23°\mathrm{C}$ and $T = 100°\mathrm{C}$ in a Ni–Zn ring sample. Symbols: fluxmetric method. Solid line: coaxial line method.

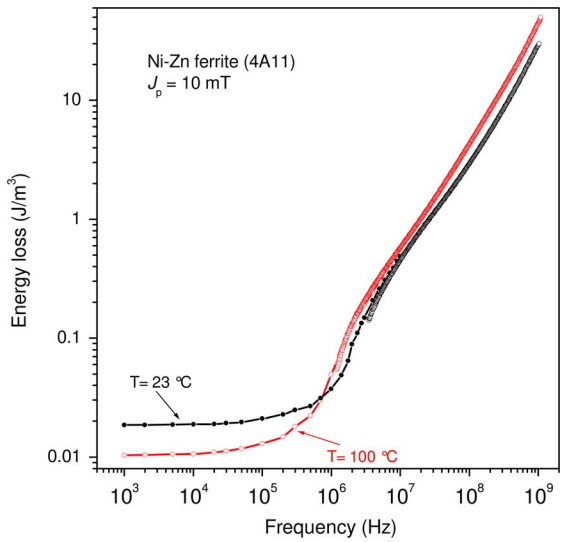

Fig. 6. Energy loss $W(f)$ versus frequency at $T = 23°\mathrm{C}$ and $T = 100°\mathrm{C}$ in the Ni–Zn ring sample of Fig. 5.

curve by extrapolation to $f = 0$. They also generate, on a different spatial scale, the dynamic dissipation effects, whose description relies, according to the classical experiments of Dillon and Earl in Mn ferrite single crystals [14], on the equation for the damped motion of the 180 ° DW

$$2J_s(H_a - H_c) = \beta_{sd}\dot{x} \tag{2}$$

describing the proportionality relationship between the wall velocity $\dot{x}$ and the dynamic field $(H_a - H_c)$, the difference between the applied field H_a and the pinning field H_c. J_s is the saturation magnetization and the damping coefficient β_{sd} is given by $\beta_{sd} = (2J_s/\mu_0\gamma\delta)\cdot\alpha_{\mathrm{LL}}$, with γ the electron gyromagnetic ratio and δ the DW thickness [15]. Starting from (2), one can generalize the statistical theory of losses [16] to the case where dissipation mechanisms other than eddy currents operate. As already demonstrated [10], such a theory permits one to analytically relate the DW generated dynamic loss $W_{\mathrm{dyn,dw}}(f)$ to W_h and consequently predict the total DW loss $W_{\mathrm{dw}}(f) = W_h + W_{\mathrm{dyn,dw}}(f)$. Therefore, we arrive at the results like the one shown in Fig. 7, where the predicted $W_{\mathrm{dw}}(f)$ behaviors at 23 °C and 100 °C in the Mn–Zn ferrite are put in evidence. It is apparent in this figure that the DW processes cannot account for the high-frequency losses, which are ascribed to rotations. The imaginary DW permeability and $W_{\mathrm{dw}}(f)$ are related according to $\mu''_{\mathrm{dw}}(f) = W_{\mathrm{dyn,dw}}(f)/(\pi H_p^2(f))$, where $H_p(f)$ is the frequency-dependent peak field value at given J_p. The so obtained $\mu''_{\mathrm{dw}}(f)$ is well approximated by a standard relaxation dispersion formula, from which the real component $\mu'_{\mathrm{dw}}(f)$ can be directly derived and the contribution of the DWs

to the magnetization process can be obtained. The magnetization rotations, which are easy processes in these materials, can be described through the linear Landau–Lifshitz–Gilbert (LLG) equation, by which expressions for the real and imaginary susceptibility components are found [17]. We assume that the very complex combination of the magnetocrystalline and demagnetizing field contributions to the effective internal anisotropy fields can be lumped into a suitable distribution function, leading to a distribution of resonance frequencies [18]. A gamma-type distribution function for the local effective field $\Gamma(H_k) = AH_k^b \exp(-H_k/H_0)$, with A a normalization constant, $b = 2 - 2.3$, and H_0 a constant, is appropriate. The real and imaginary rotational permeabilities $\mu'_{\rm rot}(f)$ and $\mu''_{\rm rot}(f)$ are thus obtained from the LLG equation and suitably averaged over the distribution $\Gamma(H_k)$ and the isotropic spatial distribution of the effective easy axes [10]. The corresponding loss contribution $W_{\rm rot}(f)$ is obtained applying (1). It is shown by the dashed–dotted lines in Fig. 7, which are calculated for $\langle H_k \rangle$ passing from 150 A/m at room temperature to about 90 A/m at 100 °C. The total predicted loss is then calculated, at both temperatures as $W(f) = W_{\rm dw}(f) + W_{\rm rot}(f)$ (solid lines in Fig. 7). We remark that the loss prediction can be extended far beyond the 10-MHz range shown in Fig. 7, on the far side of the ferromagnetic resonance spectrum, by further assuming that $\alpha_{\rm LL}$ increases to some extent with the frequency [19].

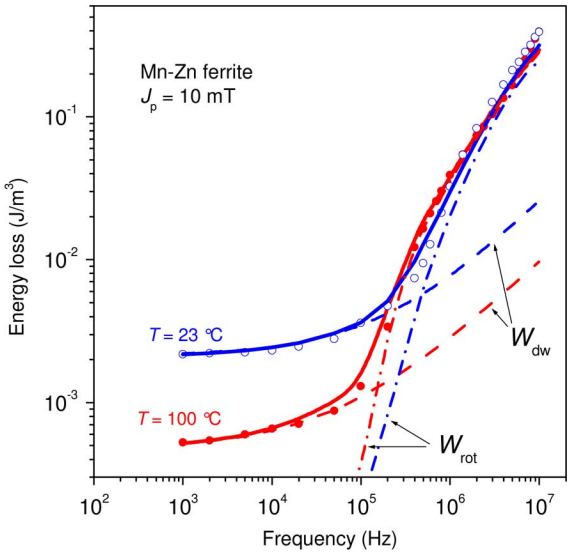

Fig. 7. Experimental loss $W(f)$ at $T = 23°$C and $T = 100°$C in the Mn–Zn ferrite (symbols) and its prediction (lines). The solid lines are obtained as $W(f) = W_{\rm dw}(f) + W_{\rm rot}(f)$, the sum of the predicted contributions from DW processes and rotations.

IV. Conclusion

The wideband loss and permeability properties of soft ferrites and their dependence on temperature are quantitatively assessed by separate appraisal of the DW processes and the rotations. To this end, the basic conceptual results of the statistical theory of losses are generalized to the case where dissipation mechanisms other than eddy currents are dominant. The DW and rotational contributions to loss and permeability are then separately achieved and their temperature dependence is accounted for. A changing temperature, besides obvious effects on the DW energy, engenders an evolution of the spectral density of the resonance frequencies for the rotations, thereby affecting the related energy absorption spectrum.

References

[1] H. Pascard, *J. Phys. IV (France)*, vol. 8, pp. 377–384, 1998.
[2] J. A. Fujita and S. Gotoh, *J. Appl. Phys.*, vol. 93, pp. 7477–7479, 2003.
[3] O. Inoue, N. Matsutani, and K. Kugimiya, *IEEE Trans. Magn.*, vol. 29, pp. 3532–3534, 1993.
[4] J. J. Suh, B. M. Song, and Y. H. Han, *IEEE Trans. Magn.*, vol. 36, pp. 3402–3404, 2000.
[5] V. T. Zaspalis, M. Kolenbrander, R. Guenther, and P. van der Valk, in *Proc. ICF-9*, San Francisco, CA, 2004, pp. 579–584.
[6] M. Drofenik, A. Znidarsic, and I. Zajc, *J. Appl. Phys.*, vol. 82, pp. 333–340, 1997.
[7] W. A. Roshen, *IEEE Trans. Magn.*, vol. 43, pp. 968–973, 2007.
[8] D. Stoppels, *J. Magn. Magn. Mater.*, vol. 160, pp. 323–328, 1996.
[9] C. Beatrice and F. Fiorillo, *IEEE Trans. Magn.*, vol. 42, pp. 2867–2869, 2006.
[10] F. Fiorillo, C. Beatrice, O. Bottauscio, M. Chiampi, and A. Manzin, *Appl. Phys. Lett.*, vol. 89, p. 122513, 2006.
[11] F. Fiorillo, *Measurement and Characterization of Magnetic Materials.*. San Diego, CA: Elsevier, 2004, p. 409.
[12] R. B. Goldfarb and H. E. Bussey, *Rev. Sci. Instrum.*, vol. 58, pp. 624–627, 1987.
[13] O. Bottauscio, M. Chiampi, and A. Manzin, *J. Magn. Magn. Mater.*, vol. 304, pp. e746–e748, 2006.
[14] J. F. Dillon and H. E. Earl, Jr., *J. Appl. Phys.*, vol. 30, pp. 202–213, 1959.
[15] J. Smit and H. P. J. Wijn, *Ferrites.*. Eindhoven, The Netherlands: Philips Technical Library, 1959, p. 107.
[16] G. Bertotti, *IEEE Trans. Magn.*, vol. 24, pp. 621–630, 1988.
[17] J. C. Peuzin, , E. du Trémolet de Lacheisserie, Ed., *Magnétisme*. Grenoble, France: Presses Universitaires, 1999, vol. II, pp. 155–211.
[18] P. Gelin, P. Queffelec, and F. Le Pennec, *J. Appl. Phys.*, vol. 98, 2005, 053906.
[19] F. Fiorillo, M. Coïsson, C. Beatrice, and M. Pasquale, *J. Appl. Phys.*, vol. 105, 2009, 07A517.